



琉球大学学術リポジトリ

University of the Ryukyus Repository

Title	Construction of Apparatus for NQR Experiment
Author(s)	Niki, Haruo; Ikushima, Yasuo; Kikuchi, Yasuhide; Igei, Ryokan
Citation	琉球大学理学部紀要 = Bulletin of the College of Science. University of the Ryukyus(36): 27-51
Issue Date	1983-09
URL	http://hdl.handle.net/20.500.12000/12548
Rights	

Construction of Apparatus for NQR Experiment

Haruo NIKI*, Yasuo IKUSHIMA**, Yasuhide KIKUCHI** and Ryokan IGEI*

Abstract

Apparatus for NQR experiment was constructed and its performances were tested. The apparatus includes a temperature controller whose performance was tested by observing the resonance line of ^{35}Cl in a sample, NaClO_3 , while its temperature was controlled in the range from 77 K to about 300 K. It was found that during the measurement the temperature of the sample was controlled within ± 0.2 K. A microcomputer was introduced in accumulating the weak signals and its effectiveness is discussed.

§1 Introduction

Since the observation of Dehmelt and Krüger¹⁾ on the nuclear quadrupole resonance(NQR) of chlorine nucleus in trans-dichloethylene in 1950, a number of NQR experiments on molecules of many substances have produced fruitful results.

Here we will give a brief explanation of the NQR, details of which will be found in many published papers.^{2,3,4,5)} The NQR arises from the variation of electrostatic interaction between the electric charges of an atomic nucleus and its surroundings. In a nucleus of spin $I \geq 1$, the distribution of its positive electric charge is not spherically symmetric but of ellipsoid in classical analog. In such a state, the nucleus has an electric quadrupole moment, an analog of nuclear magnetic moment. If the positive nuclear charge is located in the electrostatic field of external charges as shown in Fig.1, then the state of Fig. 1(b) will be stabler than that of Fig. 1(a) because of an electrostatic interaction, meaning that the energy state resulted from electrostatic interaction will depend on the orientation of the nucleus. Even for the present case, the orientation of the nucleus is not arbitrary but limited and therefore the corresponding energy states can arise only in certain limited manners. For example, in the cases of chlorine nuclei ^{35}Cl and ^{37}Cl , whose nuclear spins are $I = 3/2$, there are four energy levels ($2I + 1$) but only two levels are distinct because of the symmetry of the nuclear electric charge distribution (reversing the direction of the nucleus will not result in different electrostatic energy). Upon applying electromagnetic wave equivalent to the energy difference between the two levels, the quadrupole moment occupying the lower level will be induced to the upper level, changing its orientation. This is the principle of NQR.

Received: May 14, 1983.

* Department of Physics, Division of General Education.

** Graduating senior physics major, College of Science.

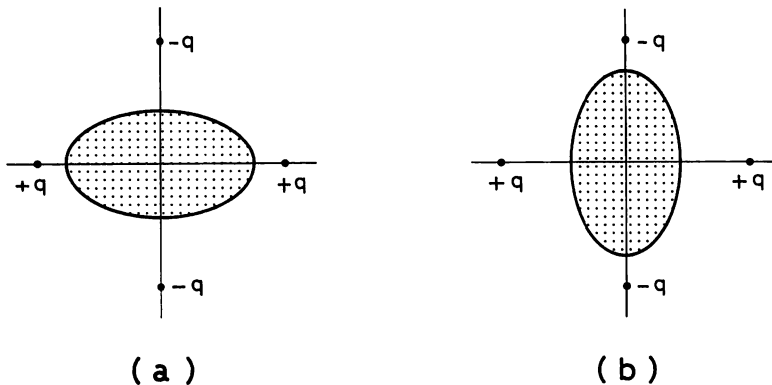


Fig. 1. Dependence of energy levels upon the nuclear orientation due to the point charges surrounding the nucleus. The state of (b) is stabler than that of (a). Here, the q is positive.

The NQR of a nucleus depends on the charge distribution around the nucleus, and when the distribution is of higher symmetry than that of cubic, the nuclear energy level will degenerate and NQR will not be observed, but for the charge distribution of lower symmetry than that of cubic, an electric field gradient due to the deviation from cubic symmetric distribution of the surrounding charge exists at the position of the nucleus and the degeneracy of the energy level will be partially removed, enabling one to observe NQR. Since the electric charge surrounding the nucleus can be considered to consist of neighboring ionic charge in addition to the extra-nuclear electronic charge, the NQR observation will make it possible to investigate the degree of symmetry of the electric charge configuration surrounding the nucleus.

Since the temperature control of a sample of interest will play an important role in the study of solid by NQR experiments, we have decided to construct an apparatus for NQR experiment whereby the temperature of the sample can be controlled in the region, where we mostly perform our experiments, ranging from near liquid nitrogen point to room temperature. The construction of the NQR apparatus with temperature controller and testing its performance will be described in subsequent sections.

In conclusion, it is affirmed that the apparatus we constructed has sensitivity and temperature controlling performance sufficient for our proposed experiment for now.

§ 2 Construction of a Spectrometer for NQR Experiment

2-1 Detection of NQR line by continuous wave method

Two methods, continuous wave and pulse methods, are utilized in apparatus for NQR experiments. Though their merits are comparable, we have constructed a spectrometer based on the general continuous wave method. In this device sensitivity will be determined by the oscillating-detector which produces a radio frequency (rf) field and detects the

resonance absorption. Since the NQR absorption signal is extremely weak, how to design and control the device will become the most important problem.

In NQR experiments, regenerative and super-regenerative oscillators which make sweeping easy are used. The regenerative oscillator, so-called marginal oscillator, produces relatively low output power and is easy to control. This makes the oscillator most suitable for the study of the substances whose relaxation time is long and therefore whose resonance lines saturate fast. The marginal oscillator is superior to the super-regenerative one regarding the observation of the shape of resonance line and separation of close resonance lines. On the other hand, since the super-regenerative oscillator can produce high oscillating power with high sensitivity, it is utilized in the study of substances whose relaxation time of resonance line is of no problem. We constructed the regenerative oscillators because we mostly deal with the substances whose resonance shape we observe and whose resonance lines saturate fast.

In NQR experiments, the resonance signals are modulated at low frequency and the resulted alternating signals are amplified and recovered after detecting the amplified alternating signals through a phase sensitive detector(PSD). Two techniques exist for modulation: frequency modulation(FM) and magnetic field modulation(Zeeman modulation). We mostly used the former and left the latter for trial only.

Next, the signal detection using the FM technique will be described. First, a rf field is applied to the sample. Then, the central frequency of the modulated rf field is slowly swept and once the rf field sweeps the resonance frequency, an absorption corresponding to the shape of the resonance line will take place, and as a result, the amplitude of the rf field will be modulated by the modulating field. The component of the amplitude will be picked up as signal and detected. The situation is shown in Fig. 2. Here, when the range of frequency modulation is narrower than the width of the resonance line shape, the detected signal becomes the 1st derivative of the resonance line as shown in the lower part of Fig. 2. After detecting the rf fields, only the low frequency components were amplified. At this stage, the resonance can be observed over an oscilloscope only when the signal is very intense: otherwise the signal is masked by noises and can not be observed. The improvement of the signal-to-noise ratio (S/N) is accomplished by using a lock-in amplifier which performs three functions: narrow band amplification which amplifies only the modulated frequency component, phase-sensitive detection which takes a modulating frequency as reference signal, and rectification which rectifies the signal through filters. The signal thus rectified is recorded. Further improvement of S/N will necessitate accumulating process. This process is carried out by feeding the signals first into an analog-digital (A/D) converter and then into a microcomputer. The block diagram of the circuits for what have been described above is shown in Fig. 3. In the subsequent sections will follow the explanation of the circuits with attention paid to their construction.

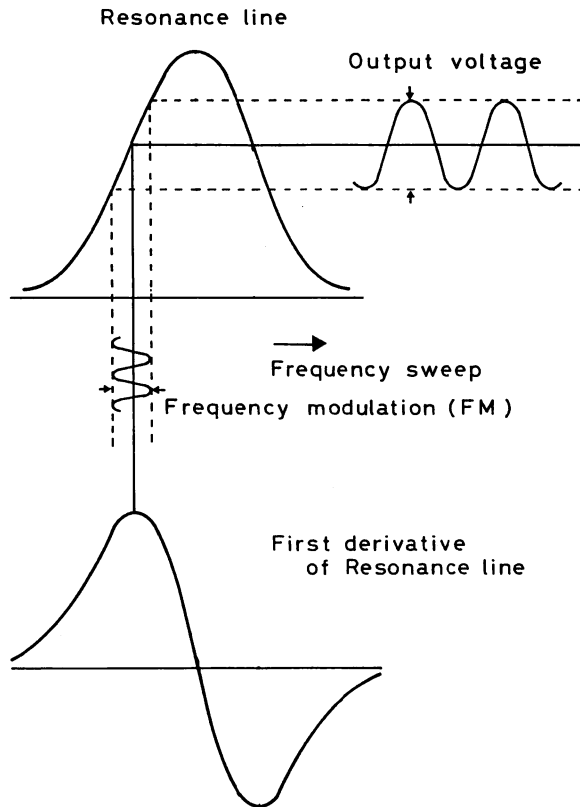


Fig. 2. Diagram illustrating the detection of resonance line by frequency modulation (a) Absorption line (b) The 1st derivative of the absorption line.

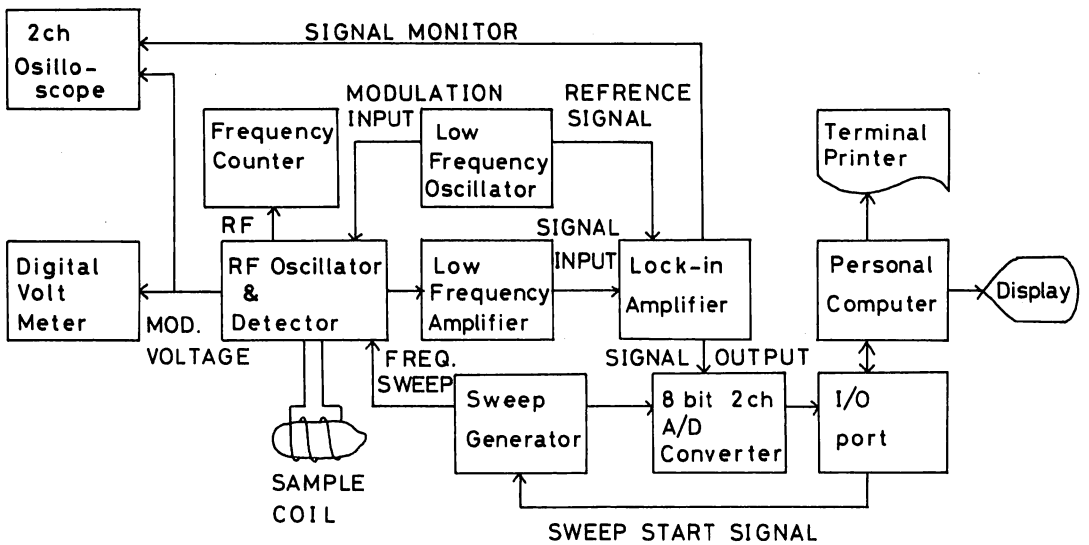


Fig. 3. Apparatus for NQR experiment using continuous wave method.

2-2 Construction of regenerative oscillating-detector

We constructed several regenerative oscillating-detectors including ones with different methods of exciting^{6,7)}. Out of these oscillators, we will describe one which is easy to adjust. The circuit of this oscillator is shown in Fig. 4. The values of the circuit elements of these oscillators are determined to give frequency range from 20 MHz~30MHz, but by varying them it is possible to obtain frequency range from a few MHz~above 30 MHz. The essence in arranging a rf frequency circuit is to make the circuit compact by making the leads to earth as short as possible. This necessitates careful arrangement of parts.⁸⁾ Otherwise the circuit may not yield an expected performance. Taking this into consideration, we made the rf frequency part and preamplifier (low frequency amplifier) compact and housed them in a metal shield-case in order to prevent the leakage of the rf frequency field and to shield external noises. Diagrammatic sketch of the existing parts in the shield-case is given in Fig. 5. The leads for power source and signals were let out of the shield-case through filtering condensers which were directly connected to the shield-case. In order to attenuate rf frequency fields, the lead from power source was again carefully shunted with by-pass condenser inside the shield-case. Because of easiness in soldering, stainless steel plate was used for the shield-case. Copper plate might be better if magnetic shielding is unnecessary.

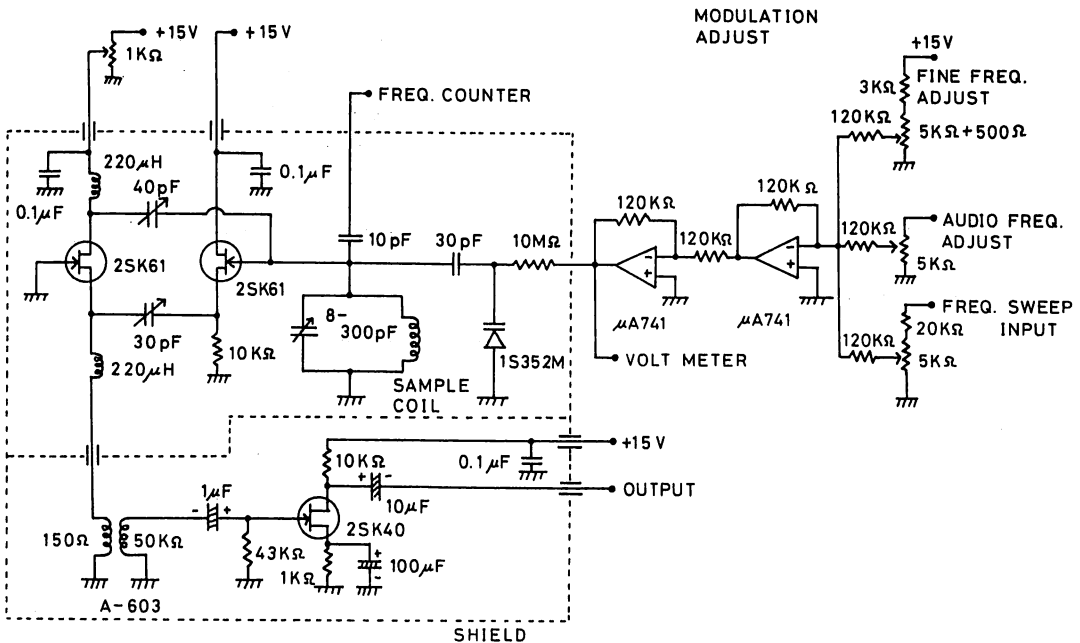


Fig. 4. Marginal oscillating-detector circuit. The values of the circuit elements are for the frequency range 20~30 MHz.

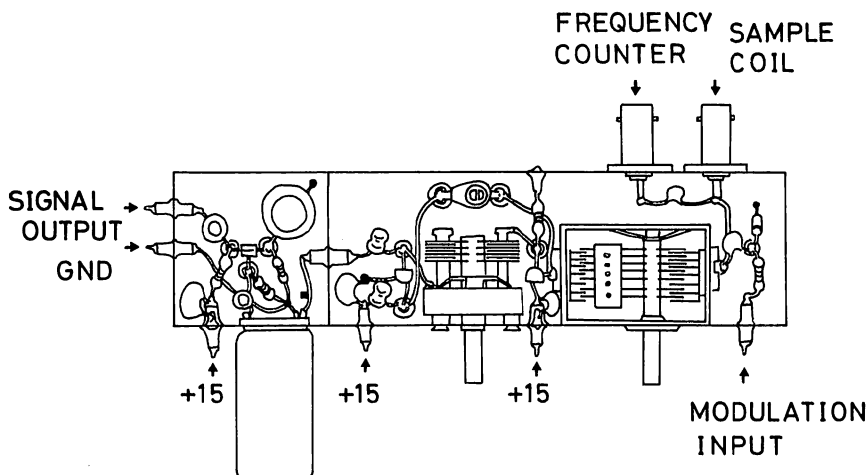


Fig. 5. Diagrammatic sketch for the oscillating-detector part of the marginal oscillating-detector.

Next, circuit elements will be described. Because of easy access and low noise figure (NF), we chose 2SK61 (Toshiba) for field effect transistor(FET). In semiconductors such as FET, some fluctuation in performance is not unusual even among the products of the same specification. Therefore we checked many 2SK61 and chose ones with good performance. Since variable air condenser performs stabler than trimmer condenser, we used the former wherever mounting was no problem. Ceramic condensers were used for high frequency field. Since resistors can become a source of noise, it is advisable to use metal-coated resistor whenever accessible. The high frequency circuit was coupled to preamplifier at a transformer, a commercial product (Sansui A-603) which is doubly shielded magnetically.

2-3 Frequency modulation

The frequency modulation circuit shown in Fig. 4 is an operational amplifier designed as a summing amplifier. By applying as a bias voltage the sum of voltages of frequency modulation, frequency sweep, and fine adjustment across a diode of variable capacitance(varicap), the capacitance of the varicap is varied. The capacitance variation of the varicap, which is connected in parallel to the LC resonance circuit including the sample coil, will result in change of the effective capacitance of the resonance circuit, leading to variation of resonance frequency. According as whether the bias voltage is a.c. or d.c. the output is of frequency modulated or of constant frequency. In continuous wave method, frequency sweep must be done simultaneously with frequency modulation. Since a d.c. voltage of constant period must be applied, saw-tooth or triangular wave of long period must be utilized. Though the LC circuit is adjusted by varying capacitance, the fine adjustment which can not be done by directly varying the capacitance is realized by varying the d.c. voltage applied to the varicap.

As the varicap, 1S352M was used, and the bias voltage applied to the varicap was varied in the range of 6~8V since it was used in the linear portion of the frequency change for the voltage of the resonance circuit. The modulating voltage impressed as the bias voltage of the varicap is sinusoidal wave of about 100Hz~1kHz in frequency and a few mV~100mV in amplitude. This is equivalent to several kHz ~several 10 kHz when converted to modulation frequency width. In order to keep frequency-sweep to sweep-time ratio constant, the width of the sweep frequency was held to a few kHz ~30kHz. The sweep time was from 100 seconds to a few minutes and the sweeping speed, though it depends on sweep width, was from 3 to 10 sec/kHz.

2-4 Improvement of signal-to-noise ratio(S/N)

The signal detected by a spectrometer usually includes many noises. A lock-in amplifier serves to improve the S/N. The lock-in amplifier we used is LI-544A(NF product). The name "lock-in" amplifier originates in its function whereby it "locks" the phase of the input at the phase of a reference signal which has the same frequency with that of the signal of interest.

The ordinary lock-in amplifier consists of a narrow band amplifier, a phase sensitive detector(PSD), and a low-pass filter. It is adjusted with the reference signal whose frequency is equal to that of the signal of interest. The narrow band amplifier amplifies the fields whose frequencies lie within a narrow band whose central frequency is set equal to that of the signal of interest. Therefore, the fields whose frequencies lie outside the band will be filtered out when they pass through the narrow band amplifier. Next, the outputs of the narrow band amplifier are fed to PSD which is synchronized with a reference signal whose frequency and phase are set equal to those of the signal of interest. So, the output consists of the rectified signal of interest and a.c. noises. Finally, by letting them pass through a low-pass filter of an appropriate time constant, only the component of the signal of interest will be picked up with its S/N improved. The PSD rectifies the fields whose frequencies are equal to that of the reference signal and its rectified output is proportional to the cosine of the phase difference between the reference signal and input signals. When the input signal is in phase with the reference signal, the output is positive and when out of phase negative. When the input signal is out of phase with the reference signal by 90° or 270°, there will be no output. Therefore, though the noise is of the same frequency with that of reference signal, it may not be removed yet depending on its phase relation with that of the reference signal and may still be included in the rectified output. In order to attenuate the component of the noise further, the time constant is set to the extent not to disturb the signal of interest so that the S/N may be improved as much as possible.

The resonance signal whose S/N is improved by the lock-in amplifier as stated above was recorded by an X-Y recorder by applying the voltage of sweep frequency field to the abscissa(X) and the output voltage of the lock-in amplifier to the ordinate(Y). The resonance signal of ³⁵Cl in a sample, KClO₃, is shown in Fig. 6 as an example of recorded signals. The resonance signal of the sample is 20.09 MHz at room temperature.

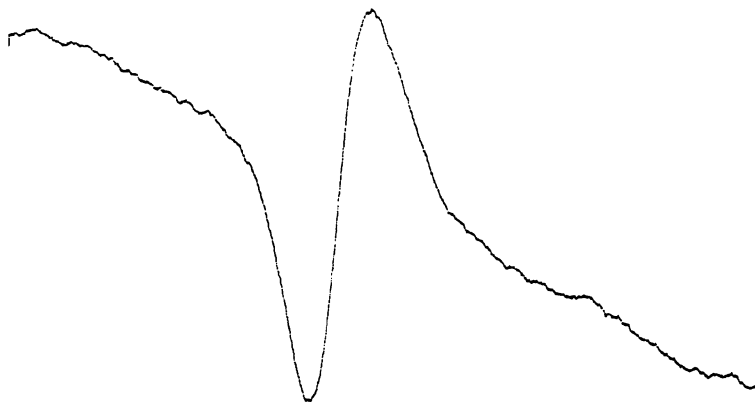


Fig. 6. Signal outputs which were sent through the lock-in amplifier.

2-5 Application of a computer to NQR experiments

Since a computer enables conversion of measured analog quantities into digital ones, the advantage of applying a computer in NQR study lies in the improvement of the S/N by treating the data whose averaging, integrating, and wave refinement are simplified by use of the computer. A computer also enables preservation and reproduction of the data. At present, a commercial microcomputer of easy access will be better for the purpose described above.

To begin with, we will describe how the output of a lock-in amplifier are fed to a computer, using the block diagram shown in Fig. 3. The analog quantities of the output signals from the lock-in amplifier are converted into digitals through A/D converter and these are in turn fed to a microcomputer at input-output (I/O) port by a command from the microcomputer. In the 8-bit A/D converter we constructed, the analog input is divided into 256 parts and converted into digital output. Though an LSI of one chip is available now, we constructed an A/D converter of comparator type: that is, we made use of a D/A converter which converts the digital output of a computer into analog, and an input analog signal was digitalized by comparing it with the output analog from the D/A converter. Its block diagram is shown in Fig. 7 with its circuit in Fig. A. 1 (see appendix). Conversion time is about 1 milisecond and error of read-in about 1 bit. The output of the lock-in amplifier and the voltage of frequency sweep were fed to A/D(X) and A/D(Y) converters, respectively, and thus digitalized each output of the A/D converters to the microcomputer.

Next, I/O port and the computer we used will be described. The I/O port is a device whereby connection between a computer and its external peripheral devices are made. Its circuit is shown in Fig. A.2. The LSI used for the I/O port is MC6821(Motorola) which is usually called PIA (Peripheral Interface Adapter). The LSI is for input-output of multipurpose, operated by a command from the computer, and has two built-in 8-bit I/O ports, each having two terminals for controlling external peripheral devices.

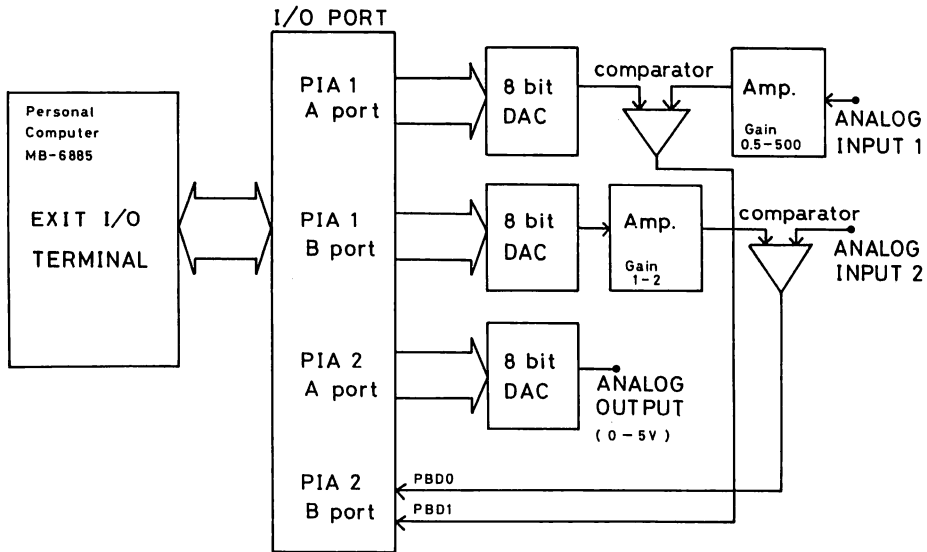


Fig. 7. Block diagram of A/D converter and I/O port.

The microcomputer we used is MB-6885 BASIC MASTER Jr. (Hitachi). Its memory capacity is 64 kByte and user's area when BASIC is used is 44 kByte. In addition to BASIC, ASSEMBLER language can also be used. With ASSEMBLER, it can perform high speed data sampling and simple data processing and with BASIC it can perform processing of high degree. The MB-6885 has two panels for graphic display with resolving power of 256 x 192. The sampling of input data can be displayed on a monitor.

The prints of output signals from various processings by the microcomputer is shown in Fig. 8. The data for one measurement is shown in Fig. 8(a). The Fig. 8(b) gives the data averaged over three measurements. It can be seen that the S/N is improved over the one for one measurement. On Fig. 8(c), the base-line is made horizontal by removing the drift of the base-line which arises due to frequency sweep and is assumed to be a straight line. The signal thus obtained makes observation easier. The Fig. 8(d) is the integral of Fig. 8(c) with respect to time. This gives reference regarding the shape of resonance line because Fig. 8(c) is the 1st derivative of the resonance line. The Fig. 8(e) is the power spectrum of the Fourier transform of Fig. 8(c). The Fig. 8(f) is the Fourier inverse of Fig. 8(e) with the high frequency components removed. Comparing Fig. 8(f) with Fig. 8(c), it is seen that minute noises are excluded. The situation above reveals the effectiveness of the data processing by a computer.

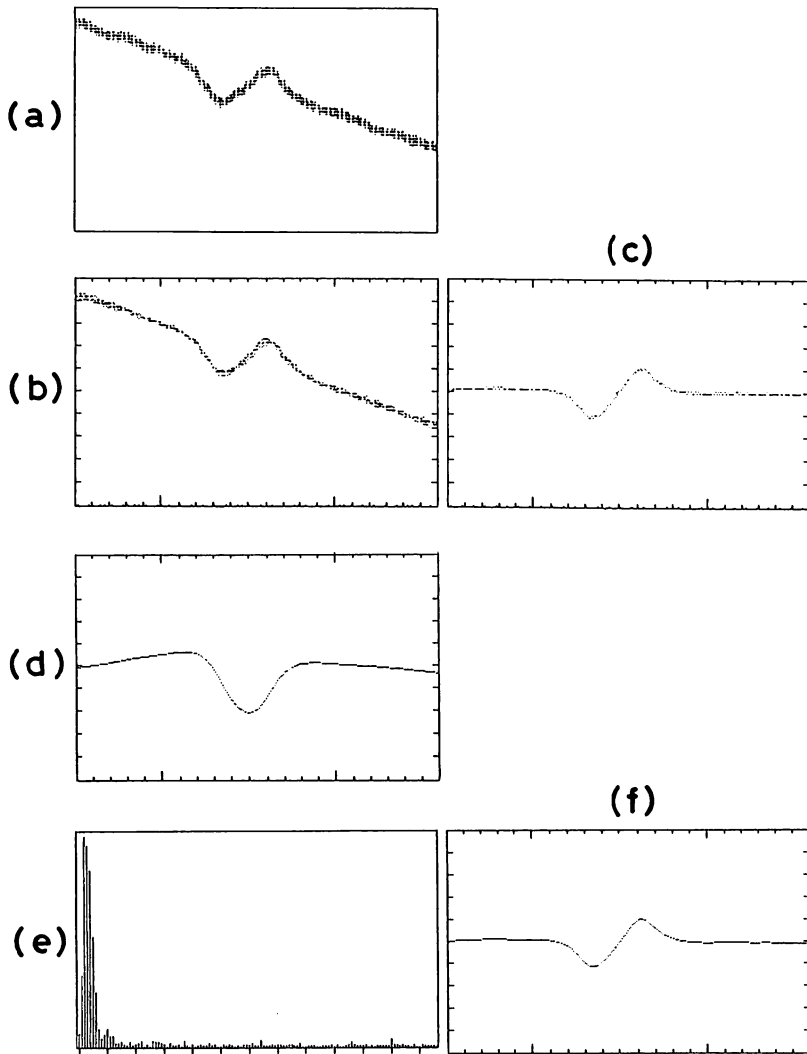


Fig. 8. Signal output processed by the computer: (a) Data of one measurement; (b) Data averaged over three measurements; (c) Base-line made horizontal by removing the assumed straight line of the base-line drift produced at frequency sweeping; (d) Integration of (c); (e) Power spectrum of the Fourier transform of (c) (The abscissa denotes frequency); (f) Inverse of Fourier transform of (e) after removing high frequency components. The abscissas of (a), (b), (c), (d), and (f) is frequency of the rf field and the unit of the ordinate is arbitrary.

§3 Construction of Temperature Controller

3-1 Cryostat

A cryostat was constructed to vary temperature from liquid nitrogen point to room temperature.^{9,10} Its schematic diagram is shown in Fig. 9. The cryostat consists of a stainless steel cylinder containing heater and Dewar vessels for liquid nitrogen. The parts excluding those of the Dewar vessels are shown in Figs. A.3-A.6, where (a) and (b) are top and side views, respectively, and the metal parts excepting that of the stainless steel are brass. The number is in millimeter unit (see appendix).

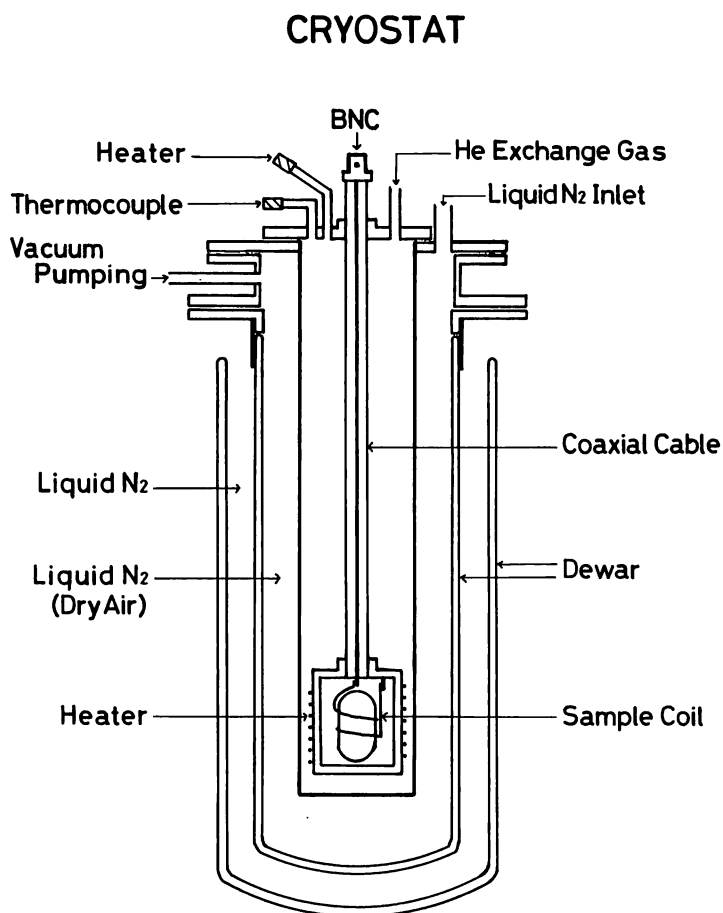


Fig. 9. Schematic diagram of the cryostat

The outer Dewar vessel is always filled with liquid nitrogen, but the inner one will be done so only in necessary temperature region to minimize heat power and thus to reduce noises in the signal. The cylinder vessel wound with heater wire is attached to the coaxial tube containing teflon as spacer and leads connected with the BNC at the top (Fig. A.3(b)).

The part shown in the diagram described above is sealed to prevent direct touch of the sample with liquid nitrogen and to avoid dew drops on the sample. Care is taken to reduce the space between the coaxial and stainless steel tubes by filling with foam styrol so that convection can be reduced. This will be explained further in next section.

The heater wire and thermocouple are put through the stainless steel tube of 8ϕ attached on the top (Figs. 9 and A.3), and the air flow is prevented by letting the leads through a plastic tube of 10 mm in diameter which is fixed with electron wax, a glue of wax type for sealing vacuum with low softening point. The cryostat is designed so that the temperature can be lowered from 77 K down to about 55 K by vacuum pumping, though it was not used in this range this time (Figs. 9 and A.5).

The enlarged diagram of the sample and its vicinity is given in Fig. 10, where the configuration of the sample, coil, and thermocouple is shown. Cylinders of brass with good heat conductivity are used to shield electromagnetic field and to obtain homogeneity in temperature.

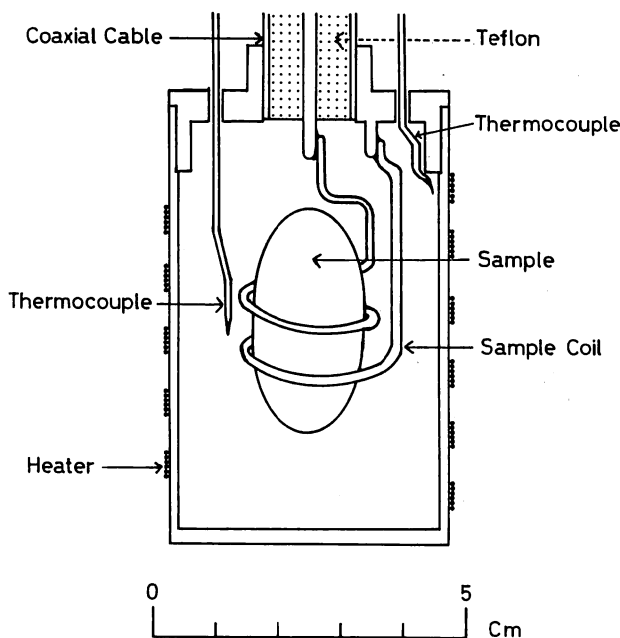


Fig. 10. Enlarged diagram of the sample and its vicinity in the cryostat.

3-2 Temperature control

The whole block diagram for temperature control is shown in Fig. 11. Copper-constantan thermocouples are used with the triple point of water as fixed point. In Fig. 11(b) the block diagram of temperature measuring device for the sample is shown. The thermocouple (Fig. 10) is connected directly to a digital voltmeter and then calibrated to give temperature readings.

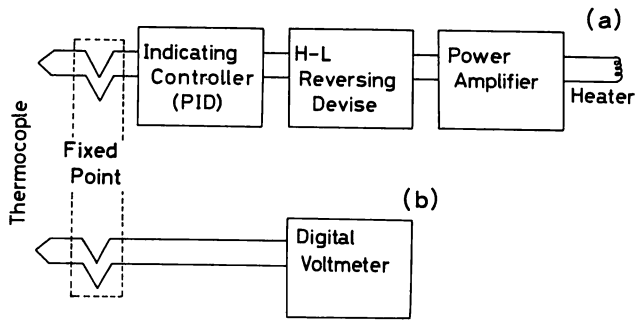


Fig. 11. Block diagram of the temperature controller: (a) Block diagram of the heater controller; (b) Block diagram for temperature measurement of the sample. The triple point of water was taken as fixed point and copper-constantan thermocouple was used.

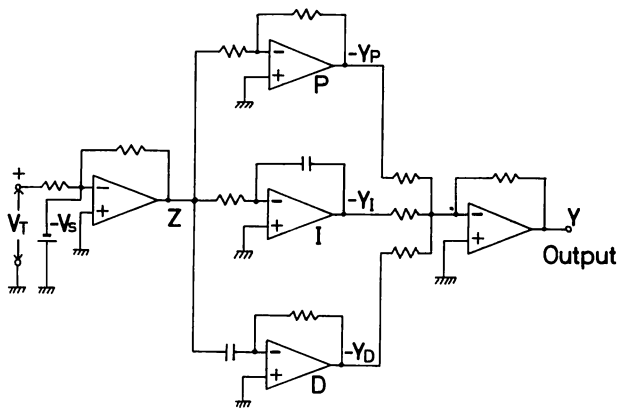


Fig. 12. PID controller circuit illustrated in simplified form. V_T : Input voltage. V_S : Set voltage. Z : Deviation voltage. Y_P : Output of proportionator. Y_I : Output of integrator. Y_D : Output of differentiator. Y : Sum of Y_P , Y_I , and Y_D .

The Fig. 11(a) is the block diagram of heater controller. The controlling device (Chino product) reads the emf of thermocouple (Fig. 10) and sends command to PID which in turn controls the heat power.^{11,12)} PID is the acronym of Proportionator, Integrator, and Differentiator.

The outline of the PID device is given in Fig. 12. The difference of input voltage of thermocouple, V_T , and the voltage corresponding to the set temperature, V_S , is fed to Proportionator, Integrator, and Differentiator. The output from these devices will be denoted by Y_P , Y_I , and Y_D , respectively. The added output, $Y = Y_P + Y_I + Y_D$, will control the heat power. The situation is shown schematically in Fig. 13. Here, when a stabilized temperature T_a is changed to a set temperature T_b at time t_a , it is assumed that the temperature adjusts

linearly with time, as shown in Fig.13(a), between t_a and t_b and that the set temperature T_b stabilizes at t_b . If the deviation voltage Z between input voltage V_T and set voltage V_S also changes linearly with time, the process will become as shown in Fig. 13(b). The Fig. 13(c), (d), and (e) represent the outputs Y_P , Y_I , and Y_D , respectively and Fig. 13(f) the output of PID which is the sum of Y_P , Y_I , and Y_D . In other words, the Fig. 13(c) represents the output proportional to Z , (d) the integration of Z with respect to time, and (e) the differentiation of Z with respect to time: that is, (c), (d), and (e) denote a straight line, parabola, and the slope of Z plotted against time, respectively.

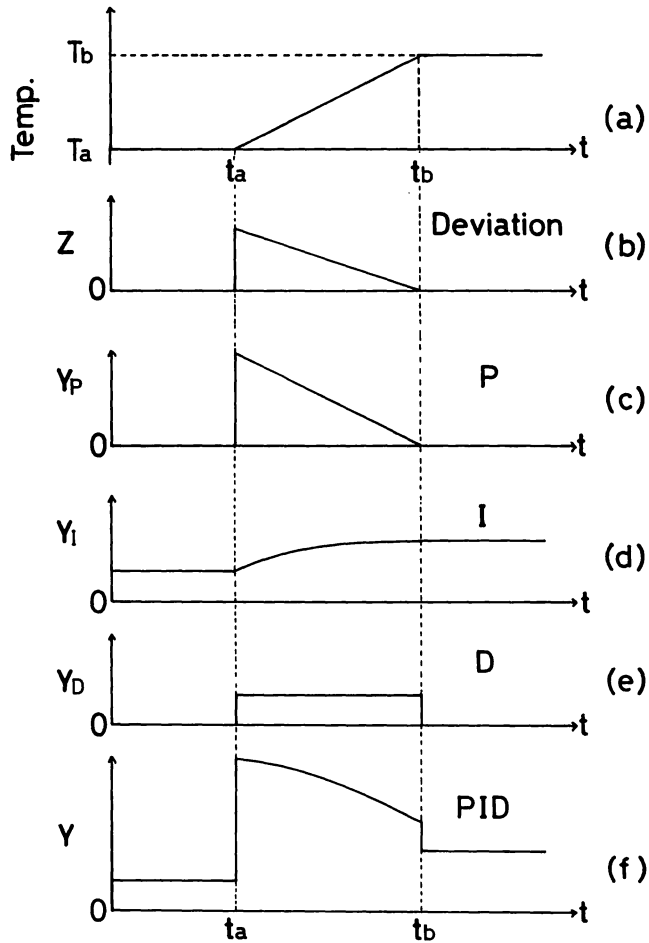


Fig. 13. Output of PID for temperature controlling. Ordinate and abscissa denote each output and time, respectively.

It is to be noted that when the deviation voltage Z stabilizes at 0, the operational output of P and D are zero but I operation yields voltage to hold the set temperature. The D operation is to make quick approach to the set temperature. What has been said are expressed in formulas as follows:

Deviation output: $Z = K_z (V_s - V_T)$.

P operation: $Y_P = K_P Z$.

I operation: $Y_I = K_I \int Z dt$.

D operation: $Y_D = K_D \frac{dZ}{dt}$.

PID operation: $Y = K_Y (Y_P + Y_I + Y_D)$.

where K_z , K_P , K_I , K_D , and K_Y are proportional constants.

The controlling device is designed such that the heat power is on or off according as whether the set temperature is lower or higher than the existing temperature: That is, the heat power is on if V_s is greater than V_T and off if V_s is smaller than V_T as shown in Fig. 14(a). These conditions are, however, for the temperature range where the set temperature is higher than fixed point. Therefore, in the region of our interest where the set temperature is lower than fixed point the polarity of the emf of thermocouple is reversed. So, in order to make proper connection to the device, the polarity of the thermocouple must be reversed. Then, when the set temperature is lower than the existing temperature, the input voltage V_T is larger than the voltage V_s corresponding to the set temperature and therefore the heat power will be off, and when the V_T is smaller than V_s the heat power will be on. Therefore, the controlling device without alteration can not control the temperature in the region of our interest (below fixed point). This necessitated us to introduce Low-High temperature inveter to reverse the way of supplying power as shown in Fig. 14 (b). The circuit for power amplifier is shown in Fig. A. 8.

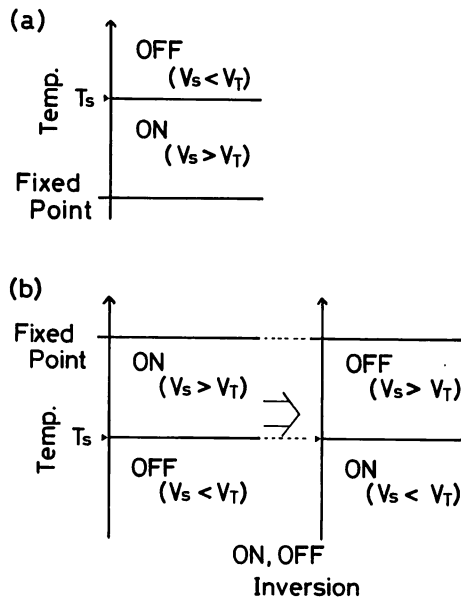


Fig. 14. Controlling translated into ON and OFF in each temperature region: (a) Controlling in the region above the fixed point; (b) Controlling in the region below the fixed point. As shown in the figure on the right, operation of the device is the reverse of that in the figure on the left. T_s : Set temperature. V_s : Voltage corresponding to the set temperature. V_T : Input voltage.

§4 Experiments and Comments

In order to see the performance of the apparatus for NQR experiments described in previous sections, we carried out experiment using sodium chlorate (NaClO_3) as a sample.^{3,13)} The sodium chlorate is a standard sample of easy access and the temperature dependence of the NQR resonance frequency of the chlorine nucleus in NaClO_3 is large.

The chlorine nucleus has two isotopes, ^{35}Cl and ^{37}Cl with percentage of abundance being 75% and 25% for the former and the latter, respectively. The difference in abundance gives no effect to the shapes of their signals; the only difference lies in the resonance frequency and the ratio of the resonance frequency is constant. Therefore, we chose the ^{35}Cl which exists more abundantly in nature than ^{37}Cl .

To begin with, an experiment was performed with the temperature controlled at about 300 K which was 10 K above the room temperature. No liquid nitrogen was put in either the inner or outer Dewar vessel. The state of the experiment is shown in Figs. 15 and 16. The Fig. 15 gives the plot of measured temperature of the sample. As the graph indicates, the temperature variation is confined to ± 0.1 K. The Fig. 16 shows the observation of the resonance frequency of NQR during the simultaneous temperature measurement above. The deviation of the resonance frequency at about 300 K is 2.5 kHz /K and taking into account the experimental error and also the deviation of the resonance frequency, the temperature deviation of the sample was found to be within ± 0.1 K.

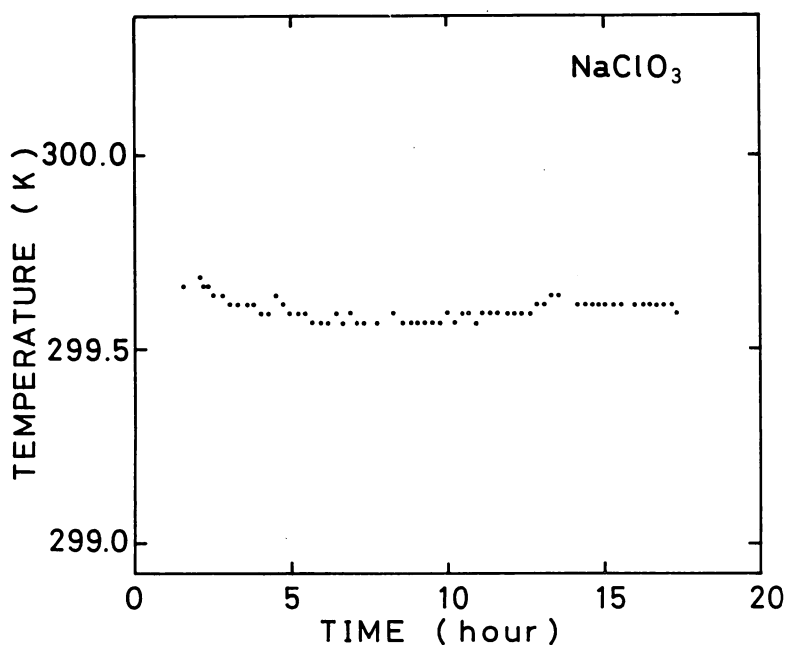


Fig. 15. Temperature variation against time of the sample NaClO_3 when controlled at 300 K.

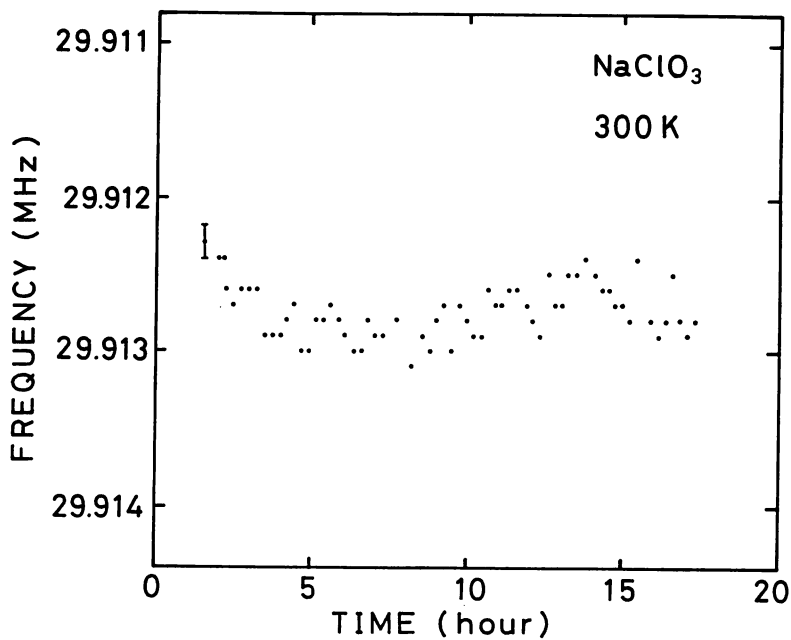


Fig. 16. Variation of resonance frequency of ^{35}Cl in NaClO_3 controlled at 300 K simultaenously measured with the data in Fig. 15.

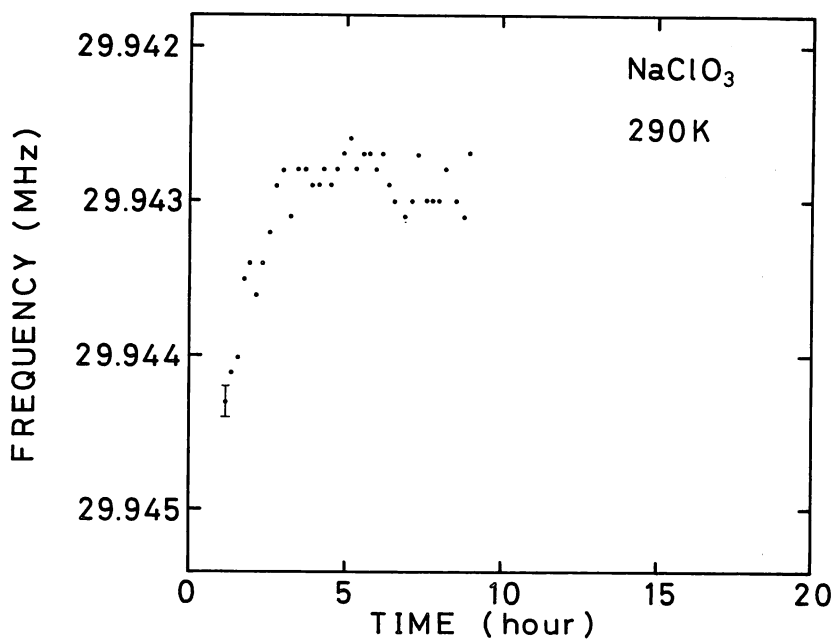


Fig. 17. Variation of resonance frequency of ^{35}Cl in NaClO_3 when the temperature of the sample was not controlled.

The Fig. 17 shows the graph for the case when the temperature of the room was left unchanged as much as possible without controlling the temperature in the device. As is revealed in this graph, it is clear that when the temperature in the device is not controlled the temperature variation is significant. Judging from these results, we think that the temperature controlling device for NQR experiment will stand sufficiently for the use in our interest.

Next, we tested our device for the performance in lower temperature region by checking the temperature dependence of the NQR resonance frequency of ^{35}Cl using the same sodium chlorate as a sample. The outer Dewar vessel was always filled with liquid nitrogen, and the inner one is filled with liquid nitrogen in the temperature range from 77 K ~ about 200 K but not in the region of about 200 K ~ about 300 K. Since the convection of helium exchange gas seemed to disturb the temperature to stabilize, we introduced pieces of foam styrol to reduce the volume of the helium exchange gas and lowered the heat leakage at the top of the cryostat as mentioned in section 3. This enabled us to control the temperature sufficiently for NQR experiment.

Proceeding with our experiment as shown in Fig.18, we obtained the temperature dependence of the NQR frequency of ^{35}Cl of NaClO_3 . About an hour was necessary to obtain the data corresponding to one spot in the Figure and during all this time the state of temperature controlling depended on the heat power of the device: the temperature variation was confined to ± 0.1 K for temperature ranges of about 77 K ~ about 150 K and about 200 K ~ about 300 K, and even for the worst case the variation was limited to ± 0.2 K which was for the region of about 150 K ~ about 200 K.

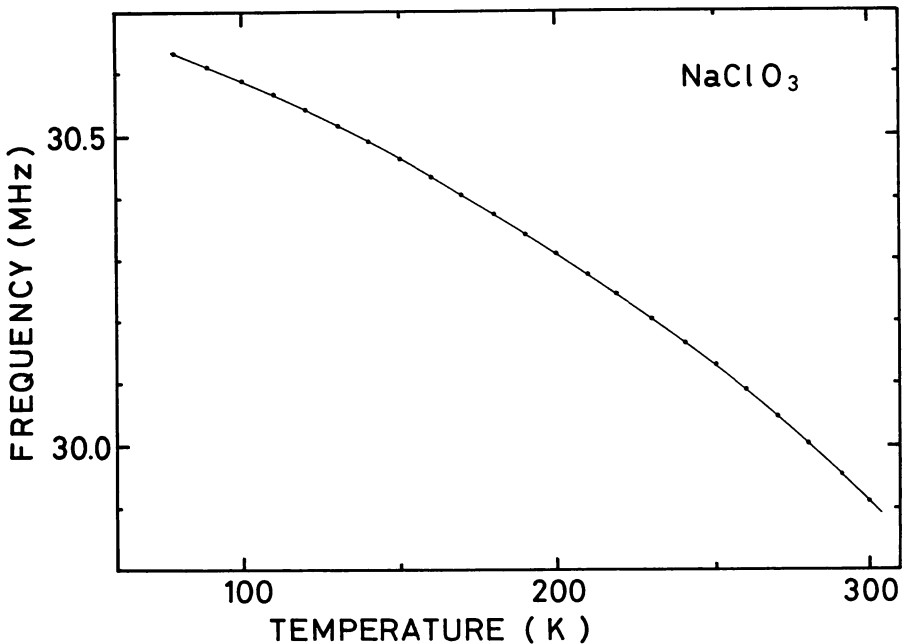


Fig. 18. Temperature dependence of the resonance frequency of ^{35}Cl in NaClO_3 .

As mentioned at the outset of this section, the ^{35}Cl of NaClO_3 is known to have wider temperature dependence of NQR resonance frequency than the chlorine nuclei in other compounds. Therefore our devices should be able to stand sufficiently for NQR experiment using other compounds as samples.

Acknowledgements

The authors would like to extend their gratitude to Mr. J. Tamashiro of Physics Department, College of Science for his advice and generous cooperation in constructing the cryostat.

Appendix

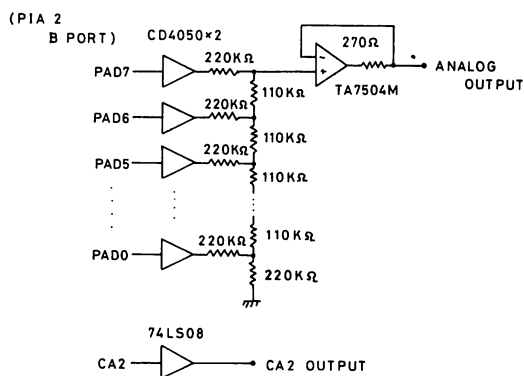
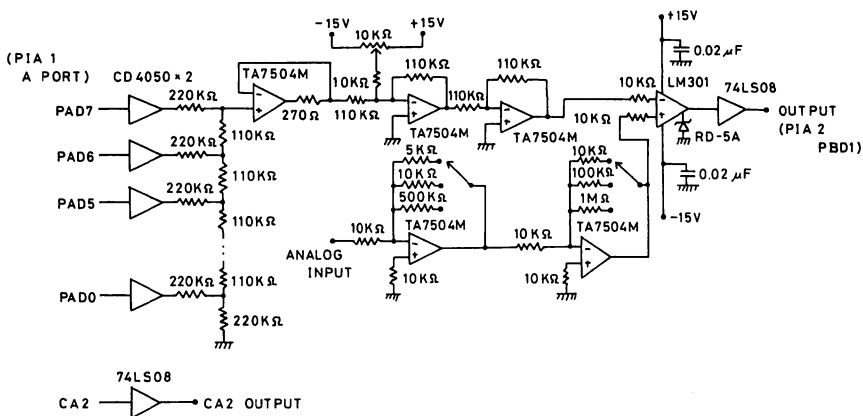


Fig. A.1. D/A converter circuit.

(a)



(b)

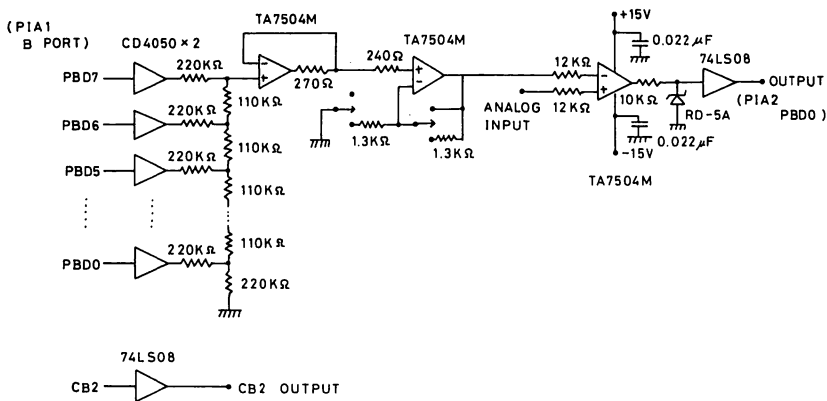


Fig. A.2. A/D converter circuit: (a) for A port of I/O; (b) B port of I/O.

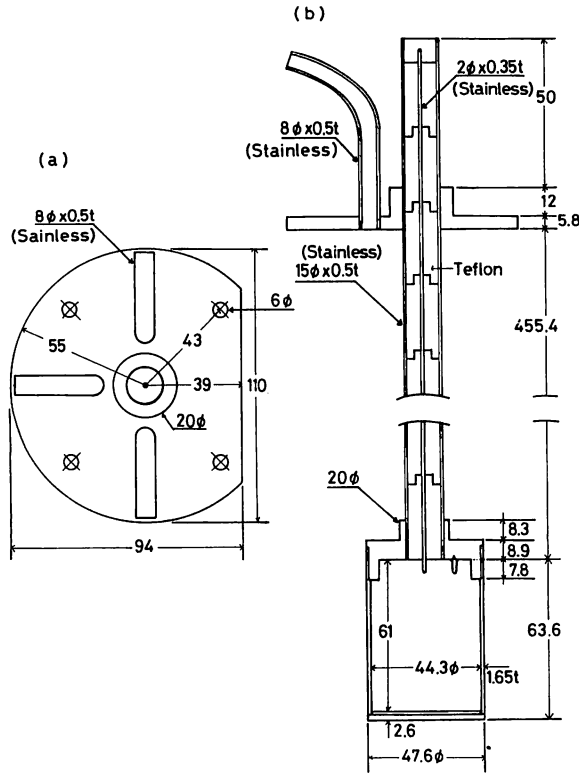


Fig. A.3. Dimension of the cryostat(I): (a) Top view; (b) Cross-sectional side view.

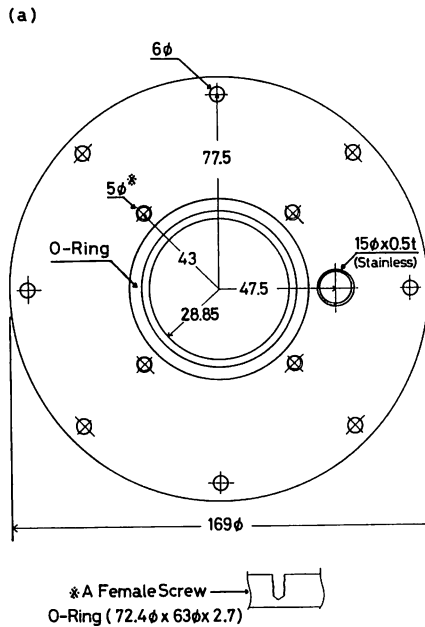


Fig. A. 4(a). Dimension of the cryostat(II). Top view.

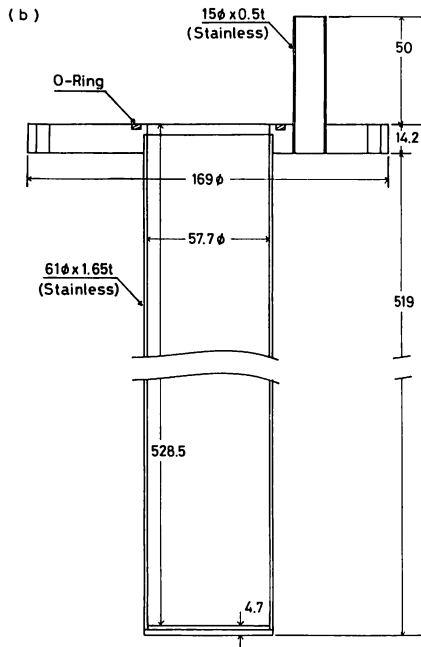


Fig. A. 4(b). Dimension of the cryostat(II). Cross-sectional side view.

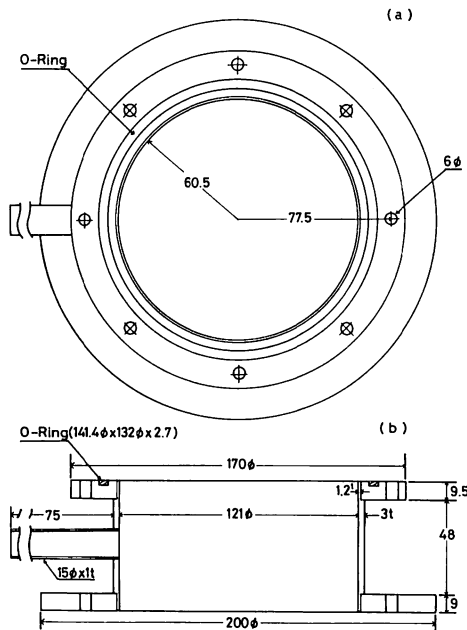


Fig. A. 5. Dimension of the cryostat(III): (a) Top view; (b) Cross-sectional side view.

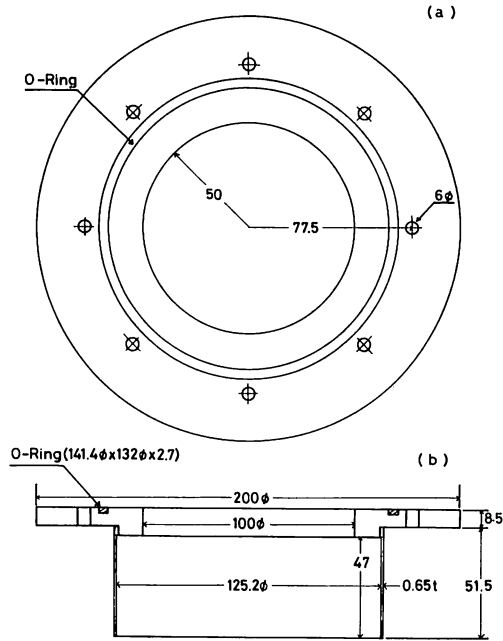


Fig. A. 6. Dimension of the cryostat (IV): (a) Top view; (b) Cross-sectional side view.

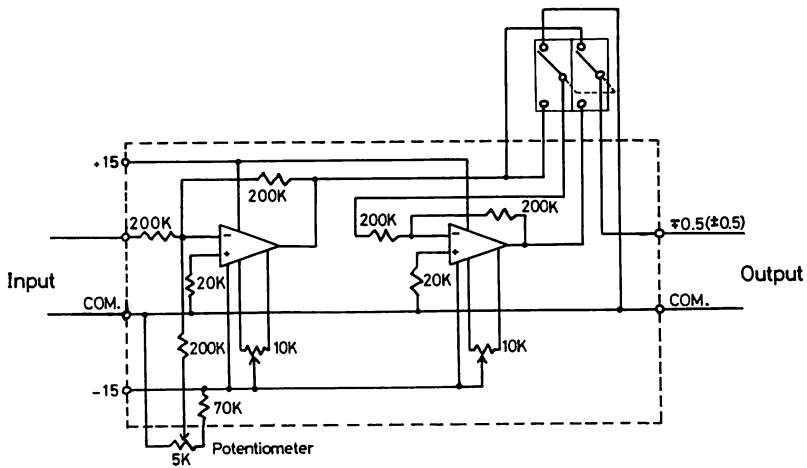


Fig. A. 7. H-L reversing diode circuit. Broken line represents print board. As the operational amplifier $\mu A741$ is used.

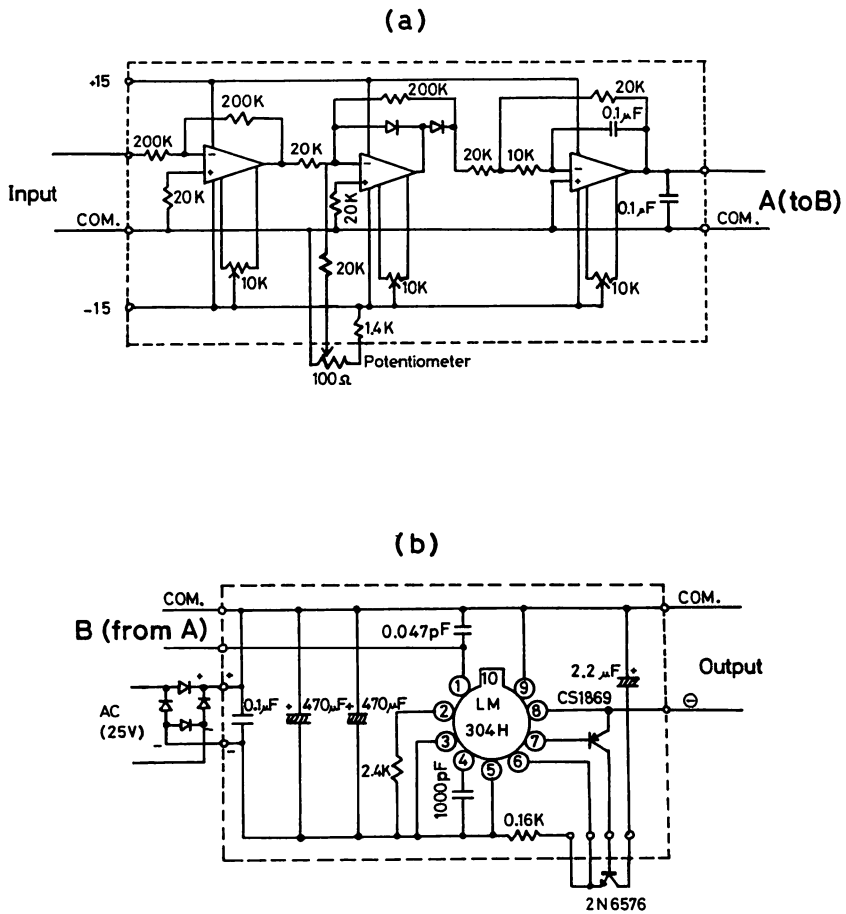


Fig. A. 8. Power amplifier circuit: (a) Input controlling part; (b) Output controlling part. Broken line represents print board. As the operational amplifier $\mu A741$ is used.

References

- 1) H. G. Dehmelt and H. Krüger: *Naturwiss.* **37**(1950) 111.
- 2) T. P. Das and Hahn: *Nuclear Quadrupole Resonance Spectroscopy*, *Solid State Physics*, F. Seitz and D. Turnbull (Academic Press, New York, San Francisco, London) Suppl. 1.
- 3) E. A. C. Lucken: *Nuclear Quadrupole Coupling Constants* (Academic Press, London and New York, 1969).
- 4) C. P. Slichter: *Principles of Magnetic Resonance* (Harper and Row, New York, 1978) 2nd ed.
- 5) D. Nakamura and R. Ikeda: *Jiki, Jikken Kagaku Kōza* ed. Nihon Kagaku Kai (Maruzen, Tokyo, 1976) *Kisogijutsu* 2, §5.3, p.458 ~492 [in Japanese] .
- 6) T. L. Viswanathan, T. R. Viswanathan and K. V. Sane: *Rev. Sci. Instrum.* **39**(1968) 472.
- 7) T. L. Viswanathan, T. R. Viswanathan and K. V. Sane: *Rev. Sci. Instrum.* **41**(1970) 477.
- 8) Y. Mizuno: *Jisshoteki Erektoronikusu Kōsaku Gijutsu* (CQ Shuppan, Tokyo, 1979) [in Japanese].
- 9) S. Tanuma: *Teion, Jikken Butsurigaku Kōza* (Kyoritsu Shuppan, Tokyo, 1974) vol. 15 [in Japanese] .
- 10) *Teion Gijutsu, Bussei Jikken Shirizu*, ed. Bussei Henshū Iinkai (Maki Shoten, Tokyo, 1968) Vol. 3 [in Japanese] .
- 11) T. Aira: *Kiso Jido Seigyo* (Morikita, Tokyo, 1978) [in Japanese] .
- 12) H. Kobayashi and T. Yoshida: *Jido Seigyo no Kisochishiki* (Ohm Sha, Tokyo, 1978) [in Japanese] .
- 13) T. Wang: *Phys. Rev.* **99**(1955) 566.